Chiral-Selective Protection of Single-walled Carbon Nanotube Photoluminescence by Surfactant Selection†

Timothy J. McDonald,‡,§ Jeffrey L. Blackburn,‡ Wyatt K. Metzger,‡ Garry Rumbles,‡ and Michael J. Heben*,‡

National Renewable Energy Lab, Golden, Colorado 80401, and Department of Applied Physics, Columbia University, New York, New York 10027

Received: February 19, 2007; In Final Form: August 3, 2007

We study the effects of adding H_2O_2 to acid-purified and unpurified single-walled carbon nanotubes (SWNTs) in aqueous suspensions using photoluminescence (PL) and optical absorption spectroscopies. The addition of H_2O_2 to suspensions of unpurified SWNTs results in a rapid (1−2 h) quenching of the photoluminescence from all tubes, whereas H_2O_2 addition to acid-purified SWNTs causes the nanotube PL to grow in intensity over a period of several days before decaying in a tube-specific manner that depends on the binding strength of the surfactant sheath. With the appropriate choice of surfactants, the PL for specific acid-purified SWNTs can be protected such that novel mid-gap and phonon-assisted absorption and emission transitions can be observed without the obscuring effects associated with emission from other nanotubes. The H_2O_2 treatment also results in a reduction of the high-energy absorption background that has been associated with either carbonaceous impurities or the SWNT π-plasmon oscillation. An understanding of the related mechanisms leads to a new method for separating nanotubes by type based on selective oxidation followed by selective precipitation. These findings offer the possibility of efficiently separating large quantities of nanotubes by chirality.

Introduction

Since the discovery of band gap luminescence from single-walled carbon nanotubes (SWNTs) in 2002,[1] interest in these novel one-dimensional molecular materials for photonic[2−5] and photoconversion[6−8] applications has accelerated. A major impediment to the widespread application of SWNTs has been the polydispersity in nanotube band gap inherent in current synthesis methods.[9] Though synthetic methods can produce samples with reduced diameter distributions,[10] there is currently no high-yield technique for controlling nanotube chirality. In this paper, we report a novel and simple chemical processing method that selectively quenches the photoluminescence (PL) from all but a single nanotube type in a distribution. The processing is based on the observation that surfactants bind to SWNTs with a strength that can be chirality- and diameter-dependent.[11] Nanotubes with strongly bound surfactant species are protected to some degree against chemical reaction. Chemical processing that affects all but the protected tube can be used to enhance the PL of the protected tube while dramatically reducing and, in some cases, eliminating, the PL background from other species. Consequently, the normally congested PL excitation landscape seen for SWNT distributions in solution can be simplified so that subtle new phenomena may be observed and quantified. The protected tube may also be selectively precipitated from solution and then re-suspended in a separate solution. This latter approach is a new, potentially scalable method for separating nanotubes according to (n,m) index.

Methods and Discussion

Previously, we demonstrated that certain surfactants exhibit selective interactions with specific nanotube types in aqueous solutions.[11] For example, sodium dodecyl sulfate (SDS) binds more strongly to small diameter nanotubes, and the binding strength varies smoothly with diameter. In contrast to SDS, sodium cholate (SC) binds strongly to certain nanotube types, such as the (7,5) nanotube, and weakly to other nanotubes with almost the same diameter, such as the (10,2) nanotube. Thus, the SC binding dependence is chiral-selective rather than diameter-dependent. Other studies have shown that nanotubes suspended by bile salts, such as sodium cholate, have greater buoyancy in suspensions during ultracentrifugation.[12] The most buoyant nanotubes that fractionate near the top during density-gradient ultracentrifugation are those that bind most strongly to the surfactant. In this work, we utilize the fact that the surfactant sheath surrounding specific nanotubes is more robust and can provide protection against chemical oxidation initiated by hydrogen peroxide.

We employed both raw (unpurified) and purified SWNTs produced by high-pressure decomposition of carbon monoxide (HiPco),[13] as well as purified SWNTs grown by decomposition of CO on cobalt−molybdenum catalyst (CoMoCat).[10] The as-received purified nanotubes were acid purified by their respective suppliers. Solutions were prepared by combining 20 mg of SWNT material and 15 mL of D_2O containing either sodium cholate (SC, 1 wt %) or a mixture of SC (1.6 wt %) and sodium dodecyl sulfate (SDS, 0.4 wt %). The latter surfactant mixture was recently shown to permit SWNT separations during density gradient centrifugation.[12] The mixtures were agitated by cup-horn sonication with a Cole Parmer 750 W homogenizer at 30% power for 15 min and then sonicated overnight in a Branson

† Part of the special issue "Richard E. Smalley Memorial Issue".

* To whom correspondence should be addressed. Email: michael_heben@nrel.gov.

‡ National Renewable Energy Lab.

§ Columbia University.

10.1021/jp071410d CCC: $37.00
Published on Web 10/18/2007

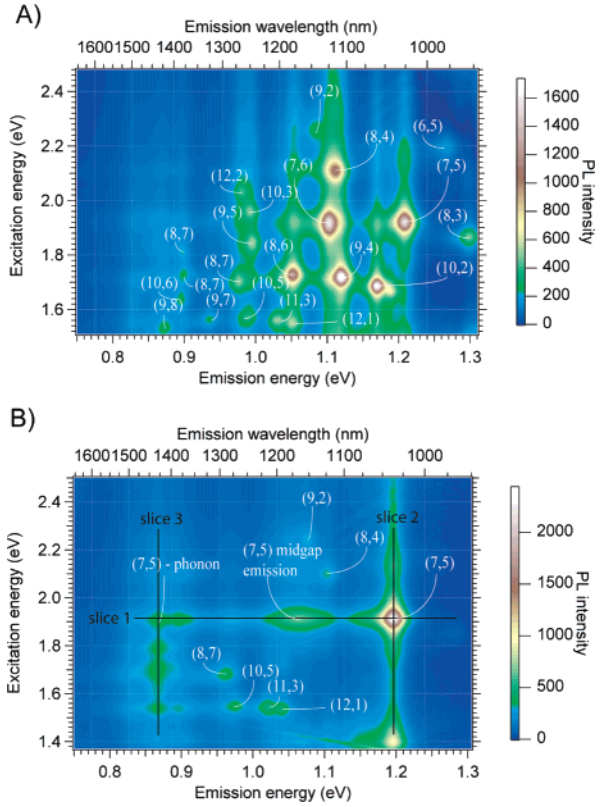

Figure 1. Excitation versus emission PL contour maps of (A) purified HiPco SWNTs suspended by sodium cholate and (B) the same suspension added to an equal part of H_2O_2 after 7 days. Many new phonon-assisted absorption and emission features are present in panel B, as discussed in the text and the Supporting Information.

2510 ultrasonic bath. A final cup-horn sonication at 100% power followed immediately by ultracentrifugation at 122 000 g removed large SWNT bundles from the suspension. This process produces suspensions having single and relatively small bundles of tubes that are stabilized against agglomeration by adsorbed surfactant species.[1] The resulting suspensions are stable for many months.

Excitation versus emission PL maps were measured with a customized Thermo-Electron FT960 Raman spectrometer equipped with a Ge detector operating at 77 K.[14] The excitation source was a 250 W tungsten−halogen bulb coupled to a single-grating monochromator. All spectra were corrected for intensity variations in the lamp spectrum as well as for the response of the FT system and detector. Time-dependent changes in the PL intensity of individual nanotubes were measured by stepping the monochromator to the excitation maximum of each nanotube of interest and collecting the emission spectrum from each selected tube every few seconds, as previously described.[14] Optical absorption measurements were performed with a Cary 500 double-beam spectrometer at a spectral resolution of 1 nm in 1 cm cuvettes. As previously described,[15,16] time-correlated single-photon counting was performed with photoexcitation at the E_2 wavelength provided by an optical parametric amplifier pumped by the output of a titanium−sapphire laser system with a regenerative amplifier. The emission was passed through long-pass filters and a spectrometer tuned to the E_1 wavelength and was detected by a cooled (80 K), infrared-sensitive photomultiplier tube.

Figure 1A shows the PL map of a typical suspension of purified HiPco SWNTs isolated by SC (1 wt %) in D_2O. Over 30 different individual semiconductor nanotube types are observed and their (n,m) indices can be assigned following Weisman et al.[17,18] After mixing the suspension with an equal part of H_2O_2 (30% v/v, Sigma Aldrich) and waiting 7 days, the PL map was dominated by the (7,5) nanotube, and emission from all other nanotubes was substantially quenched (Figure 1B). As a result, several novel emission features associated with the (7,5) tube were observed, including the coupling of phonons to both absorption and emission transitions, as well as a mid-gap emission (vide infra). The phonon-assisted absorption transitions in the excitation spectrum are evident in slice 2 of Figure 1B, whereas the phonon-assisted emission processes are seen in slice 1. For example, the emission seen at ~0.87 eV upon excitation at ~1.92 eV corresponds to luminescence from a state that is lower in energy than the E_1 state at ~ 1.2 eV by the energy of the G′ mode, or two D phonons (~2650 cm^{-1}). Interestingly, this particular emissive state is excited effectively by multiple excitation energies (slice 3), which can be correlated to absorption processes that couple the absorption of a photon and the simultaneous emission of one or more phonons. Several other recent reports have explored phonon-assisted transitions in the absorption[15,19−24] and emission processes,[22] but the majority of these reports examine excitation of the SWNTs with photon energies that exceed the E_1 or E_2 energy by one or more discrete phonon energies.[15,19−22,24] To our knowledge, a rich emission spectrum such as that shown in Figure 1B, involving multiple phonon-assisted emission peaks, has not been seen before. A more complete discussion of these phonon-assisted transitions is included in the Supporting Information.

The PL of the (7,5) tube was "selected" from the congested PL landscape shown in Figure 1A when either purified HiPco or purified CoMoCat SWNTs were suspended in SC and treated with H_2O_2 but not when suspensions containing unpurified, or raw, SWNTs were treated in the same manner. To understand this finding in more detail we collected PL versus time data for several different SWNT species in 1% SC solutions at various temperatures. Figure 2A shows the time-dependent PL decay for unpurified HiPco tubes after addition of H_2O_2 at room temperature (22 °C). The PL emission is reduced by more than 50% within 1 h, and the suspended nanotube material flocculated and precipitated completely in a few days. Unpurified nanotubes contain significant amounts of residual metal particles left over from the SWNT synthesis. These metal impurities and related ionic species can catalytically decompose H_2O_2 to produce hydroxyl radicals ($HO^{\bullet}$) via Fenton's chemistry.[25] In a recently developed purification process for HiPco tubes, Wang et al. asserted that strongly oxidizing $HO^{\bullet}$ radicals produced by Fenton's chemistry were responsible for the destruction of SWNTs in the absence of acid.[26] The dispersions of unpurified SWNTs examined here may be subject to the same reaction, with the additional possibility that the surfactant species we employed may also be attacked by $HO^{\bullet}$. Note that the same rapid PL quenching shown in Figure 2A was observed whenever H_2O_2 was added to any dispersion we formed from raw nanotubes using SC, SDS, SDBS (sodium dodecyl benzene sulfonate), or ssDNA (single-strand DNA) as surfactants. Song et al.[27] reported the bleaching of the E_{1-} optical absorption transitions on a somewhat longer time scale (~4 h) when SDS-encased, unpurified HiPco tubes were exposed to H_2O_2 at concentration below 200 ppm. Their findings agree with our results because PL emission is much more sensitive than optical absorption to changes in surface chemistry (vide infra). The mechanism could not be completely specified, but electron withdrawal (hole injection) due to peroxide adsorption or the formation of hydroperoxides[28] was suggested.[27]

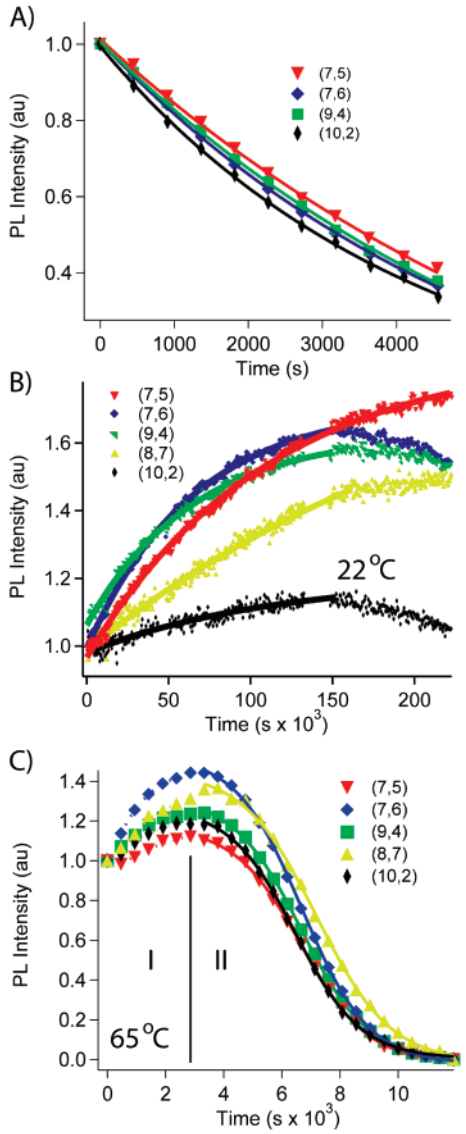

Figure 2. Photoluminescence intensity versus time for emission from single nanotubes in SC (1 wt %) suspensions treated by adding H_2O_2. The suspensions contain (A) raw, unpurified HiPco SWNTs at room temperature, (B) purified HiPco SWNTs at room temperature, and (C) purified HiPco SWNTs at 65 °C. The PL intensity from each nanotube has been normalized to unity at time = 0. Regions labeled I and II in panel C correspond to regions of PL increase and decay, respectively. The solid lines in panels A and B and the dotted lines in panel C are single-exponential function fit to the data points. The solid lines in C are fit sigmoid functions. The gap in data in panel B at 140,000 s shows when the Ge detector briefly became too warm to respond during collection over 2.5 days.

Figure 2B shows the PL versus time data for an SC suspension of purified HiPco tubes after addition of H_2O_2 at room temperature. Upon introducion of H_2O_2, the PL intensity for all tubes slowly increases with time. Similar experiments conducted with purified HiPco tubes using other surfactants (i.e., SDS, SDBS, or ssDNA) exhibited relatively rapid PL decay like that shown in Figure 2A. Thus, the use of SC and purified SWNTs is essential to observe the initial increase in the PL signals. After ~2.5 days, the PL from the (7,5) tube is still increasing whereas the PL from all other tubes has begun to decrease. After 7 days of reaction, the PL map shown in Figure 1B is obtained. Note that the PL increase in Figure 2B for purified SWNTs occurs on a time scale that is 50 times longer than the PL decay shown in Figure 2A for unpurified SWNTs. The purification process, though proprietary, is known to involve exposing the raw materials to acids (typically HCl or HNO_3) to remove accessible metal species by dissolution. As a result, the purified HiPco SWNTs have significantly bleached E_1 absorption transitions and dramatically quenched PL intensities relative to dispersions prepared with raw HiPco SWNTs, as expected for protonation of nanotube sidewalls.[29,30] The residual acid is evidently strongly bound to the SWNT surfaces because the pH of solutions prepared from the purified HiPco SWNTs is near 7.

The purified, surfactant-stabilized, and centrifuged SWNTs are expected to have very low metal concentrations, but, surprisingly, transmission electron microscopy (TEM) images of the suspended nanotubes (see Supporting Information) showed that metal catalyst particles were still abundant. The many observed particles were greater than 1 nm in diameter, and it is likely that smaller particles are present as well. Knowing that residual metal particles and acid species are present in the suspensions made from purified SWNT samples, we can consider explanations for the PL increase with time. Because the acidic species are bound, we cannot propose that the remaining metal particles are dissolved into solution, which would reduce the opportunity for catalytically produced $HO^{\bullet}$ to interact destructively with the SWNT surfaces, as suggested by Wang et al.[26] Applying a somewhat different argument, we consider that the adsorbed protons with associated counterions[31,32] are able to afford a degree of protection to the SWNTs against radical attack by quenching $HO^{\bullet}$. The radical chemistry is expected to be quite complicated, especially if Cl, S, or N species are present as acid counterions,[33] and a detailed analysis of the related surface chemistry is beyond the scope of this report. However it seems clear that the initially protonated SWNTs are protected against $HO^{\bullet}$ attack in a manner that depends on the (n,m) index until the degree of protonation, which suppresses the PL, is reduced. With further reaction, the PL from each tube is subsequently quenched in a manner that once again depends on the (n,m) index, perhaps via the formation of epoxide or hydroperoxide species as has been reported by Dukovic et al.[28] or by the simple adsorption of unreacted peroxide.[27] The (7,5) tube is the slowest to react in the SC system, so its PL is kinetically preserved, whereas the PL from all other tubes has been strongly or completely quenched.

It is experimentally difficult to follow the complete evolution of the PL map from Figure 1A to Figure 1B at room-temperature because of the need to keep the Ge detector temperature at 77 K and the instability of the tungsten−halogen lamp when operated continuously over a 7 day period. To reduce the time associated with the experiment we elevated the temperature of the solution. Figure 2C shows the evolution of the PL from several different nanotube species over a period of ~3 h at 65 °C. Here, we clearly see an initial increase in the PL for each nanotube (region I) followed by a period of PL decay (region II). As indicated previously, the mechanism for PL increase (region I) is likely associated with the removal of surface bound acid species, whereas the PL decay (region II) is likely due to tube oxidation and related charge injection processes that proceed once the tubes are deprotonated. The rate of PL increase in region I differs for each nanotube and is well fit by eq 1,

$$I_n = I_{n0}[1 - \exp(k_n t)] \quad (1)$$

where I_n is the intensity of the nth nanotube, I_{n0} is the intensity at time $t = 0$, and k_n is the rate of increase of the nth nanotube's PL. Table 1 shows the rate constants for the increase in PL at

TABLE 1: Exponential Fits to the PL Rise in Figure 2, Panels B and C

NT type (n,m)	PL increase rate at 22 °C	PL increase rate at 65 °C
(7,5)	9.0×10^{-6}	5.6×10^{-4}
(7,6)	1.5×10^{-5}	9.0×10^{-4}
(9,4)	1.5×10^{-5}	9.2×10^{-4}
(8,7)	1.1×10^{-5}	6.6×10^{-4}
(10,2)	3.7×10^{-5}	9.7×10^{-4}

both 22 and 65 °C. Note that the various nanotubes reach their peak intensities in the same order for both temperatures, indicating that the mechanistic pathway is the same in both cases.

To assess the activation energy for the PL increase we measured k_n for several tubes at various temperatures and performed an Arrhenius analysis according to eq 2,

$$k_n(T) = k_{n\infty} \exp\left(\frac{E_a}{KT}\right) \quad (2)$$

where T is the temperature, $k_{n\infty}$ is the rate at infinite temperature, E_a is the activation energy for PL increase, and K is the Boltzmann constant. In Figure 3, we plot the determined E_a values as a function of nanotube diameter (red circles, right axis). On the left axis, we show the activation energy for SC desorption versus diameter as previously determined.[11] The plot indicates that the E_a for the H_2O_2 reaction has the same chiral-selective functionality as the surfactant binding strength. This result implies that access of H_2O_2 to the nanotube surface is determined primarily by the tube-selective manner in which SC binds, that is, the rate-determining step is the penetration of H_2O_2 through the surfactant sheath. The (10,2) nanotube binds most weakly to SC and is rapidly affected by the H_2O_2, whereas the (7,5) nanotube binds most strongly to the SC and is affected more slowly.

After the protons are consumed, H_2O_2 and/or catalytically produced $HO^\bullet$ can oxidize the nanotubes as discussed in other reports.[27,28] These effects give rise to region II in Figure 2C in which the PL decay is well fit by a sigmoid function (eq 3).

$$I_n = I_{n0} - \frac{I_{n0}}{1 + \exp[r_n \cdot (t_{1/2} - t)]} \quad (3)$$

Here, r_n is the rate of decay of the nth nanotube's PL, and $t_{1/2}$ is the time where the nth nanotube has decayed to one-half of its initial intensity. Sigmoidal kinetics are indicative of a self-catalyzing reaction. We explain this behavior as follows: As the first H_2O_2 molecules come into contact with an unprotected (deprotonated) nanotube, the nanotube becomes oxidized and negatively charged. The charged nanotube no longer interacts with nearby surfactant molecules as strongly, and the associated surfactant displacement allows more H_2O_2 molecules to access and oxidize the same nanotube. As a result, the kinetics are self-catalyzing, as described by eq 3.

To summarize our model, the two key parameters for the selective enhancement of the (7,5) PL (Figure 1B) are (1) the presence of residual acid from purification and (2) a chirality-dependent reaction rate with H_2O_2 that is mediated by the tube-dependent binding strength of the SC surfactant. Residual metallic impurities may also be required if the essential reactant is $HO^\bullet$ rather than H_2O_2. Unfortunately, this issue cannot be completely resolved at this time because metal impurities appear to always be present to some degree in the as-purified samples. Nevertheless, the slowest nanotube to react with the H_2O_2 is

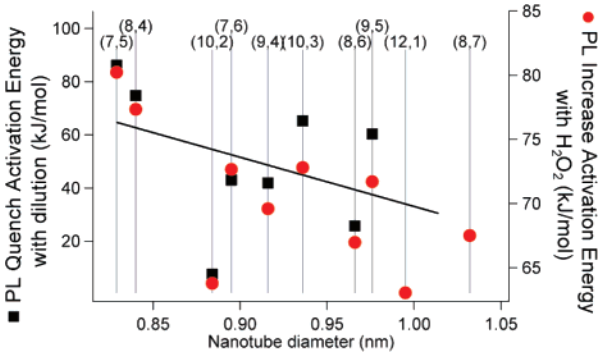

Figure 3. Red circles: Measured PL increase activation energy versus nanotube diameter for a purified HiPco suspension treated with H_2O_2. The PL increase activation energy determines how readily the H_2O_2 has access to the nanotube surface. Black squares: Measured PL quench activation energy versus nanotube diameter for nanotubes suspended by SC diluted with addition water to promote bundling in a SWNT suspension.[11] The PL quench activation energy is related to the binding strength of the surfactant molecule to each nanotube type. The solid line is a linear fit to show the deviation from pure diameter-dependent behavior.

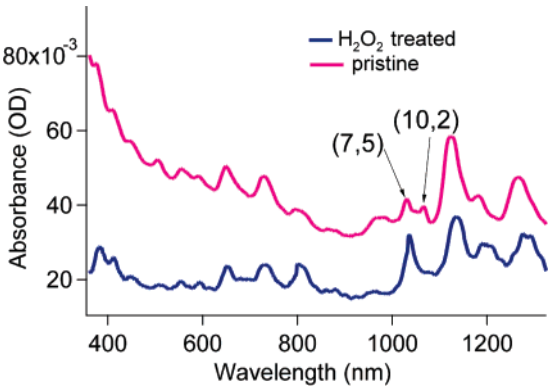

Figure 4. Linear absorption spectra of purified HiPco SWNTs suspended by SC (1 wt %) before (pink) and 7 days after H_2O_2 treatment (blue).

the (7,5) nanotube, which was previously shown to bind SC substantially more strongly than all other nanotube types (Figure 3).

Figure 4 shows the absorption spectra of purified nanotube/SC suspensions before and after 7 days of H_2O_2 treatment. Note that the rising high-energy background commonly observed for nanotube suspensions is substantially reduced by the H_2O_2 treatment. This background has been attributed to contributions from π-plasmon oscillations associated with both nanotubes and carbonaceous impurities.[34] Recent size-exclusion chromatographic studies indicate that a large portion of this high-energy rising background is likely due to persistent carbonaceous impurities.[35] Accordingly, the H_2O_2 treatment used here reduces these carbonaceous impurities.

A second thing to note is that the oscillator strength for the E_1 transition of the most strongly protected (7,5) nanotube is increased in intensity relative to the transitions for all other observed nanotubes after the H_2O_2 treatment. The PL intensity for the (7,5) tube is peaked relative to all other tubes, so it is not surprising that a sharp optical transition associated with an unprotonated species is observed.[29,30] Additionally, the optical absorptions associated with all other nanotubes besides the (10,2) species are still clearly observed. According to our analysis, the (10,2) tube binds most weakly with the surfactant and interacts most directly with the oxidizing environment. As a result, the (10,2) tube may have been severely damage or

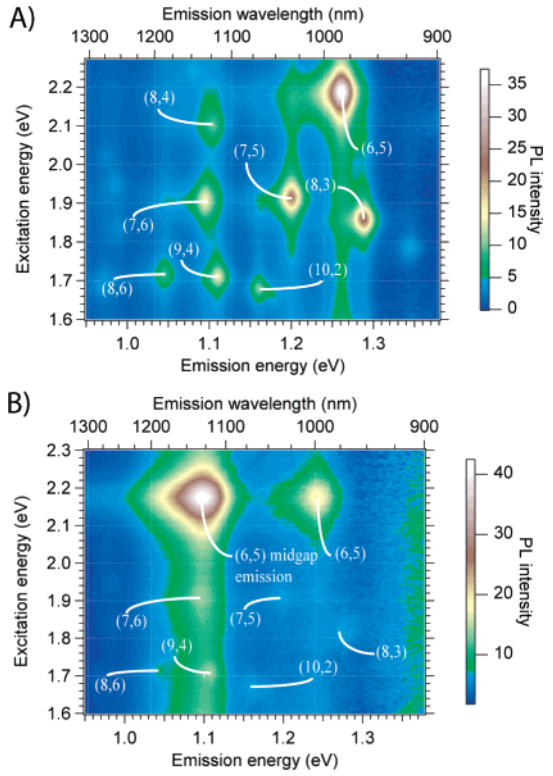

Figure 5. PL excitation versus emission contour maps of (A) purified CoMoCat nanotubes suspended by SC (1.6 wt %) and SDS (0.4 wt %) and (B) the same suspension 4 days after H_2O_2 was added.

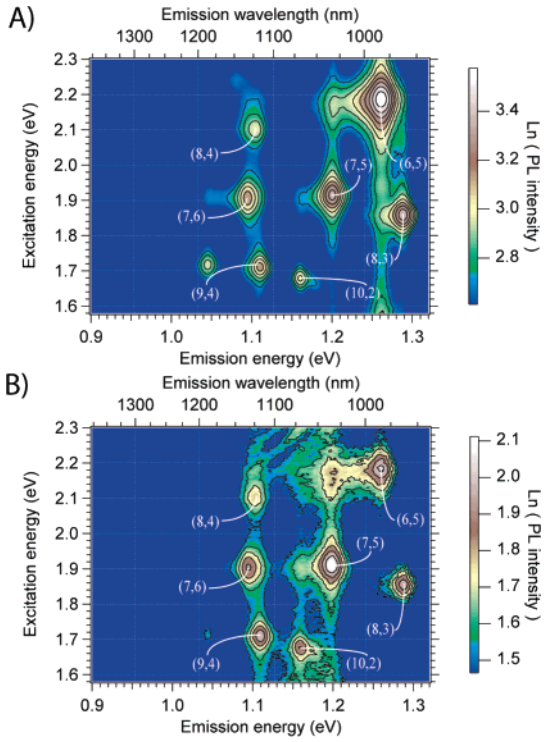

Figure 6. PL excitation versus emission contour map of (A) CoMoCat SWNTs suspended in SC (1 wt %) and (B) the same suspension treated by H_2O_2 for 7 days, with ethanol added (10% v/v), and the precipitate resuspended in SC.

digested. The fact that the optical transitions associated with all other tubes are still observed may appear to be in conflict with the PL data, but nanotube PL has been reported to be much more sensitive than optical absorption to surface chemistry associated with either protonation[29] or surface oxidation.[28] Specifically, in the case of surface oxidation,[28] the number of charges required to bleach a optical absorption transition was estimated to be an order of magnitude larger than the number required to completely quench the PL from the same transition. Qualitatively, this may be understood by considering that the intensities of the absorption spectra and the related absorption bleaching scale with the number of carbon atoms and injected carriers, respectively, whereas a single excess charge can stimulate the nonradiative recombination (i.e., quenching) of many mobile excitons. Thus, there is no discrepancy between the PL and absorption data. It is also not surprising that the nonluminescent lightly oxidized nanotubes remain suspended in solution because oxidized and charged nanotubes are known to remain stabilized against bundling and flocculation in the absence of surfactants.[36,37]

By changing the surfactants used to suspend the nanotubes, other nanotubes can be protected against H_2O_2-initiated PL quenching. Figure 5 shows the PL maps for a suspension of purified CoMoCat tubes stabilized by a mixture of SC (1.6 wt %) and SDS (0.4 wt %) before and after 4 days of exposure to H_2O_2. With this surfactant mixture the emission of the (6,5) nanotube is protected. Note that the PL of the (7,5) and (8,3) tubes has been completely quenched, whereas a strong midgap emission associated with excitation of the (6,5) tube has become clearly evident (vide infra). This result is not surprising because SDS binds most strongly to the small-diameter nanotubes,[11] and the (6,5) species is the smallest nanotube in the CoMoCat samples. The results are quite similar when HiPco SWNTs are treated in H_2O_2 with the same surfactant mixture. The addition of SDS to the solution changes the tube that is protected from the (7,5) species to the (6,5) species. Consistently, the (6,5) nanotube is also the most buoyant during separation by density-gradient ultracentrifugation with this same surfactant mixture,[12] consistent with our model. Thus, manipulation of the encapsulating surfactant sheath provides a means by which different tubes may be protected against H_2O_2-initiated reactions. This opens the possibility of finding surfactant mixtures that select other tubes besides the (7,5) and (6,5) nanotubes.

The method of protecting a specific nanotube against oxidation can be used to enhance and scale-up separations of SWNTs by type. Density-gradient separation[12] and ssDNA sorting techniques[38] result in only a small amount of material, but larger amounts of type-pure samples may be needed for many applications. The protected, luminescent nanotube requires surfactant molecules to remain suspended, whereas the reacted species can remain suspended because of the surface functional groups introduced by reaction with H_2O_2. The addition of alcohols can be used to destabilize the surfactant sheath and cause flocculation of the protected tubes. In suspensions such as those analyzed in Figure 1B (7,5-protected) or Figure 5B (6,5-protected), only a single nanotube type remains well-protected by the surfactant. When we add ethanol (10% v/v) to the suspension, only the surfactant-protected nanotube precipitates, that is, the (6,5) or (7,5) species, depending on the surfactant mixture. Subsequent ultracentrifugation and resuspension allows for enrichment of the previously protected nanotube. To demonstrate the efficacy of the approach, we prepared a suspension of CoMoCat SWNTs in 1 wt % SC. As expected for CoMoCat materials, the (6,5) PL dominates the initial PL map (Figure 6A). However, as previously discussed, the 1 wt % SC surfactant composition stabilizes the (7,5) tube. After treatment with H_2O_2 for 7 days we added ethanol (10% v/v), centrifuged, and resuspended the precipitate in SC. Figure 6B shows the PL map for the new suspension, where the (7,5) is now the most prominent nanotube in the distribution. With

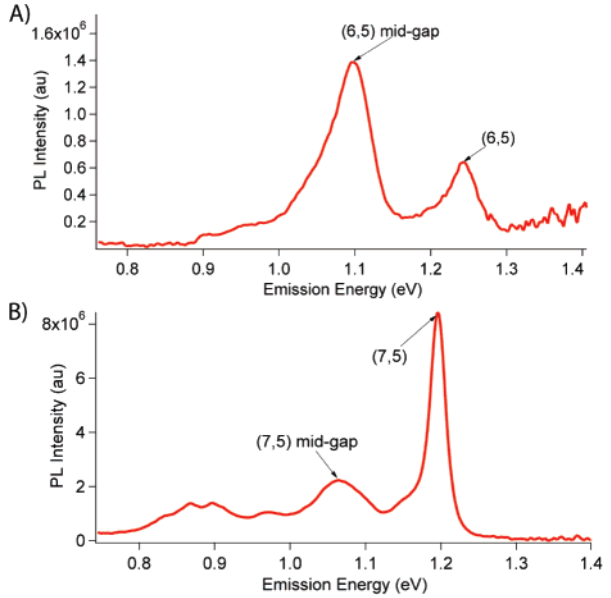

Figure 7. PL emission spectra showing midgap emission for (A) the (6,5) tube with excitation at 567 nm and (B) the (7,5) tube with excitation at 650 nm. In each, the lowest-energy excitonic transition is labeled along with an accompanying midgap emission that is observed after reaction with H_2O_2.

optimization, this method could provide a means for nanotube separation by type that is scalable, inexpensive, and environmentally benign. The use of salt concentration as an additional parameter might also be of use in this endeavor.[39]

Finally, we note that even surfactant-protected tubes may be partially oxidized by the techniques described here, leading to midgap emission as shown in Figures 1B and 5B. Figure 7 shows the emission profiles for the (6,5)-selective and (7,5)-selective surfactant combinations after the H_2O_2 treatment of CoMoCat materials with excitation into the E_2 transition for each tube (567 and 650 nm, respectively). In addition to the emission from the lowest-energy excitonic transition, there is midgap emission associated with each selected nanotube. Midgap emission has been observed previously for the (6,5) and (7,5) nanotubes at the same energies observed here, but its origin is unclear. Iakoubovskii et al. observed similar spectra after exposing nanotube/surfactant mixtures to UV light and attributed the emission to defects introduced through interactions with the surfactant molecules.[40] Alternatively, the new emission could be because of energy transfer between various nanotube types;[14,41] however, this explanation is not likely because the energy of the novel emission does not line up with any nanotube that could be considered as the recipient of the transferred energy. The midgap emission for the (7,5)-protected tube is relatively small as compared to the main emission, whereas the midgap emission is dominant for the (6,5)-protected tube; see Figure 7. This may be representative of the degree to which the two tubes may be selectively protected. To probe the nature of the midgap emission more deeply, we performed time-resolved PL on the SWNT suspension shown in Figure 5B by time-correlated single-photon counting. The time-resolved PL study of the midgap emission reveals that the lifetime of this new state is 180 ps. The lifetime is similar to that of the nanotubes' main E_1 exciton.[15,16,42] The fact that the photoexcitation relaxes from these two states in a similar manner indicates that they are strongly coupled. If the states responsible for midgap emission are the results of partial oxidation because of incomplete protection, it may be possible to eliminate them by gentle heating.

Conclusions

We report a novel method for using peroxide and the chirality-selective nature of surfactant binding to effect selective quenching of the PL from all unprotected nanotubes. The study shows that small amounts of catalytic metals used in tube growth are still present in suspensions even when previously purified SWNTs are employed. The isolation of the PL for one nanotube species allows us to observe many vibronic transitions associated with the simultaneous emission of phonons in the absorption and emission processes. In addition, we report the observation of midgap emission for two nanotube species that were selected by the surfactant interaction. The techniques described here could provide a means by which nanotubes could inexpensively separated by type.

Acknowledgment. The authors thank Gregory Scholes for helpful discussions. This work was supported by the U.S. Department of Energy (DOE) Solar Photochemistry program funded by the Office of Science, Office of Basic Energy Sciences, Division of Chemical Sciences, Geosciences, and Biosciences.

Supporting Information Available: Includes further discussion on observation of phonon coupling to transitions and TEM evidence of metal catalyst particles remaining after purification. This material is available free of charge via the Internet at http://pubs.acs.org.

References and Notes

(1) O'Connell, M. J.; Bachilo, S. M.; Huffman, C. B.; Moore, V. C.; Strano, M. S.; Haroz, E. H.; Rialon, K. L.; Boul, P. J.; Noon, W. H.; Kittrell, C.; Ma, J. P.; Hauge, R. H.; Weisman, R. B.; Smalley, R. E. *Science* **2002**, *297*, 593.

(2) Arnold, M. S.; Sharping, J. E.; Stupp, S. I.; Kumar, P.; Hersam, M. C. *Nano Lett.* **2003**, *3*, 1549.

(3) Freitag, M.; Martin, Y.; Misewich, J. A.; Martel, R.; Avouris, P. H. *Nano Lett.* **2003**, *3*, 1067.

(4) Misewich, J. A.; Martel, R.; Avouris, P.; Tsang, J. C.; Heinze, S.; Tersoff, J. *Science* **2003**, *300*, 783.

(5) Wu, Z. C.; Chen, Z. H.; Du, X.; Logan, J. M.; Sippel, J.; Nikolou, M.; Kamaras, K.; Reynolds, J. R.; Tanner, D. B.; Hebard, A. F.; Rinzler, A. G. *Science* **2004**, *305*, 1273.

(6) Guldi, D. M.; Marcaccio, M.; Paolucci, D.; Paolucci, F.; Tagmatarchis, N.; Tasis, D.; Vazquez, E.; Prato, M. *Angew. Chem., Int. Ed.* **2003**, *42*, 4206.

(7) Hasobe, T.; Fukuzumi, S.; Kamat, P. V. *J. Phys. Chem. B* **2006**, *110*, 25477.

(8) Murakami, H.; Nomura, T.; Nakashima, N. *Chem. Phys. Lett.* **2003**, *378*, 481.

(9) Haddon, R. C.; Sippel, J.; Rinzler, A. G.; Papadimitrakopoulos, F. *MRS Bull.* **2004**, *29*, 252.

(10) Resasco, D. E.; Alvarez, W. E.; Pompeo, F.; Balzano, L.; Herrera, J. E.; Kitiyanan, B.; Borgna, A. *J. Nanopart. Res.* **2002**, *V4*, 131.

(11) McDonald, T. J.; Engtrakul, C.; Jones, M.; Rumbles, G.; Heben, M. J. *J. Phys. Chem. B* **2006**, *110*, 25339.

(12) Arnold, M. S.; Green, A. A.; Hulvat, J. F.; Stupp, S. I.; Hersam, M. C. *Nat. Nano* **2006**, *1*, 60.

(13) Bronikowski, M. J.; Willis, P. A.; Colbert, D. T.; Smith, K. A.; Smalley, R. E. *J. Vac. Sci. Technol., A* **2001**, *19*, 1800.

(14) McDonald, T.; Jones, M.; Engtrakul, C.; Ellingson, R. J. *Rev. Sci. Instrum.* **2006**, *77*, 53104.

(15) Jones, M.; Engtrakul, C.; Metzger, W. K.; Ellingson, R. J.; Nozik, A. J.; Heben, M. J.; Rumbles, G. *Phys. Rev. B* **2005**, *71*, 115426.

(16) Jones, M.; Metzger, W. K.; McDonald, T. J.; Engtrakul, C.; Ellingson, R. J.; Rumbles, G.; Heben, M. J. *Nano Lett.* **2007**, *7*, 300.

(17) Weisman, R. B.; Bachilo, S. M. *Nano Lett.* **2003**, *3*, 1235.

(18) Weisman, R. B.; Bachilo, S. M.; Strano, M. S.; Kittrell, C.; Hauge, R. H.; Smalley, R. E. *AIP Conf. Proc.* **2003**, *685*, 241.

(19) Chou, S. G.; DeCamp, M. F.; Jiang, J.; Samsonidze, G. G.; Barros, E. B.; Plentz, F.; Jorio, A.; Zheng, M.; Onoa, G. B.; Semke, E. D.; Tokmakoff, A.; Saito, R.; Dresselhaus, G.; Dresselhaus, M. S. *Phys. Rev. B* **2005**, *72*, 195415.

(20) Chou, S. G.; Plentz, F.; Jiang, J.; Saito, R.; Nezich, D.; Ribeiro, H. B.; Jorio, A.; Pimenta, M. A.; Samsonidze, G. G.; Santos, A. P.; Zheng,

M.; Onoa, G. B.; Semke, E. D.; Dresselhaus, G.; Dresselhaus, M. S. *Phys. Rev. Lett.* **2005**, *94*, 127402.

(21) Htoon, H.; O'Connell, M. J.; Doorn, S. K.; Klimov, V. I. *Phys. Rev. Lett.* **2005**, *94*, 127403.

(22) Jiang, J.; Saito, R.; Gruneis, A.; Chou, S. G.; Samsonidze, G. G.; Jorio, A.; Dresselhaus, G.; Dresselhaus, M. S. *Phys. Rev. B* **2005**, *71*, 045417.

(23) Miyauchi, Y.; Maruyama, S. *Phys. Rev. B* **2006**, *74*, 035415.

(24) Perebeinos, V.; Tersoff, J.; Avouris, P. *Phys. Rev. Lett.* **2005**, *94*, 27402.

(25) Walling, C. *Acc. Chem. Res.* **1975**, *8*, 125.

(26) Wang, Y. H.; Shan, H.; Hauge, R. H.; Pasquali, M.; Smalley, R. E. *J. Phys. Chem. B* **2007**, *111*, 1249.

(27) Song, C.; Pehrsson, P. E.; Zhao, W. *J. Phys. Chem. B* **2005**, *109*, 21634.

(28) Dukovic, G.; White, B. E.; Zhou, Z. Y.; Wang, F.; Jockusch, S.; Steigerwald, M. L.; Heinz, T. F.; Friesner, R. A.; Turro, N. J.; Brus, L. E. *J. Am. Chem. Soc.* **2004**, *126*, 15269.

(29) Strano, M. S.; Huffman, C. B.; Moore, C. M.; O'Connell, M. J.; Haroz, E. H.; Hubbard, J.; Miller, M.; Rialon, K.; Kittrell, C.; Ramesh, S.; Hauge, R. H.; Smalley, R. E. *J. Phys. Chem. B* **2003**, *107*, 6979.

(30) Blackburn, J. L.; Mcdonald, T. J.; Metzger, W. K.; Engtrakul, C.; Rumbles, G.; Heben, M. J. In preparation.

(31) Zhou, W.; Heiney, P. A.; Fan, H.; Smalley, R. E.; Fischer, J. E. *J. Am. Chem. Soc.* **2005**, *127*, 1640.

(32) Hennrich, F.; Wellmann, R.; Malik, S.; Lebedkin, S.; Kappes, M. M. *Phys. Chem. Chem. Phys.* **2003**, *5*, 178.

(33) Atkinson, R. *Chem. Rev.* **1986**, *86*, 69.

(34) Itkis, M. E.; Niyogi, S.; Meng, M. E.; Hamon, M. A.; Hu, H.; Haddon, R. C. *Nano Lett.* **2002**, *2*, 155.

(35) Huang, X.; McLean, R. S.; Zheng, M. *Anal. Chem.* **2005**, *77*, 6225.

(36) Zhao, W.; Song, C. H.; Pehrsson, P. E. *J. Am. Chem. Soc.* **2002**, *124*, 12418.

(37) Chen, J.; Rao, A. M.; Lyuksyutov, S.; Itkis, M. E.; Hamon, M. A.; Hu, H.; Cohn, R. W.; Eklund, P. C.; Colbert, D. T.; Smalley, R. E.; Haddon, R. C. *J. Phys. Chem. B* **2001**, *105*, 2525.

(38) Zheng, M.; Jagota, A.; Strano, M. S.; Santos, A. P.; Barone, P.; Chou, S. G.; Diner, B. A.; Dresselhaus, M. S.; McLean, R. S.; Onoa, G. B.; Samsonidze, G. G.; Semke, E. D.; Usrey, M.; Walls, D. J. *Science* **2003**, *302*, 1545.

(39) Niyogi, S.; Boukhalfa, S.; Chikkannanavar, S. B.; McDonald, T. J.; Heben, M. J.; Doorn, S. K. *J. Am. Chem. Soc. Comm.* **2007**, *129*, 1898.

(40) Iakoubovskii, K.; Minami, N.; Kim, Y.; Miyashita, K.; Kazaoui, S.; Nalini, B. *Appl. Phys. Lett.* **2006**, *89*, 173108.

(41) Torrens, O. N.; Milkie, D. E.; Zheng, M.; Kikkawa, J. M. *Nano Lett.* **2006**, *6*, 2864.

(42) Metzger, W. K.; McDonald, T. J.; Engtrakul, C.; Blackburn, J. L.; Scholes, G. D.; Rumbles, G.; Heben, M. J. *J. Phys. Chem. C* **2007**, *111*, 3601.